IIETA International Information and Engineering Technology Association
Advancing the World of Information and Engineering

Revue des Composites et des Matériaux Avancés-Journal of Composite and Advanced Materials
Vol. 32, No. 5, October, 2022, pp. 223-228
Journal homepage: http://iieta.org/journals/rcma

Preparation of an Aluminum Titania /Mullite Composite from the Raw Materials Alumina, Titania and Silica Fume

Al-Saudi Sarah Kareem Mohammed[1,2*], Emese Kurovics[1], Jamal-Eldin F.M. Ibrahim[1], Mohammed Tihtih[1], Andrea Simon[1], Róbert Géber[1]

[1] Institute of Ceramics and Polymer Engineering, University of Miskolc, Miskolc 3515, Hungary
[2] Department of Building and Construction Technologies Engineering, Al-Eseaa University College, Baghdad 10069, Iraq

Corresponding Author Email: alsaudi.sarah@uni-miskolc.hu

https://doi.org/10.18280/rcma.320502

Received: 26 July 2022
Accepted: 27 September 2022

Keywords:
alumina, titania, silica fume, aluminum titanate, mullite

ABSTRACT

The present work deals with the preparation of ceramic composites and the study of phase transformation. Three mixtures were prepared, the main mixture containing (80 wt%) alumina and (20 wt%) titania and the other two mixtures to which two amounts of silica fume were added at (5 and 10 wt%). The phase transformation was studied at two temperatures: 1200°C and 1400°C. The X-ray diffraction results at 1200°C show that the amorphous silica (silica fume) transformed into the crystalline phase cristobalite. At 1400°C, aluminum titanate formed by the reaction of alumina with titania, and mullite formed by the reaction of alumina with silica. The result of scanning electron microscopy shows that the addition of (5 wt%) silica leads to a microstructure with smaller grain size up to (500 nm), a lower porosity (20 vol%), a lower water absorption (7 wt%) and a thermal conductivity (1.514W/m.k).

1. INTRODUCTION

Aluminum titanate (Al_2TiO_5) has many interesting properties, such as a low coefficient of thermal expansion, low thermal conductivity, and excellent thermal shock resistance because it has a high melting point of up to 1860°C [1]. Due to these advantages, aluminum titanate-based ceramics are a promising candidate for the construction of filters in hot gas purification applications and refractory materials for the automotive and non-ferrous metallurgy sectors. Aluminum titanate fibers and their nanoporous structures, on the other hand, can be used as industrial filters for purifying drinking water, as these structures effectively remove natural turbidity and other impurities [2].

Aluminum titanate material consists of one mole of aluminum oxide and one mole titania. It is formed at atmospheric pressure by heating a mixture of alumina and titania to temperatures above 1350°C [3]. However, there is a problem with this ceramic. The pure aluminum titanate is thermally unstable at temperatures between (750-1280)°C. When cooled, it tends to decompose between these temperatures, making the material unsuitable for industrial purposes. Pure Al_2TiO_5 decomposes into Al_2O_3 and TiO_2 below the equilibrium temperatureof 1300°C [4].

To obtain the solid solution structure, which should be controlled or delayed, this can be achieved by doping with oxide additives such as magnesium oxide (MgO), titanium dioxide (TiO_2), iron oxide (Fe_2O_3), zirconium oxide (ZrO_2), or silicon dioxide (SiO_2) [5].

Mullite has become an important material for basic and advanced ceramics due to its excellent mechanical and thermal properties. It has high mechanical properties at high temperatures and excellent creep resistance, which makes it suitable for use in high temperature parts [6, 7]. The low fracture toughness of mullite is usually considered an important factor limiting the possible applications that depend on this structural property. The main objective of high temperature stability requires that no glass phase is formed at the grain boundary. This is particularly difficult to achieve in mullite ceramics because the low diffusivity of the bulk and surface contributes to its high temperature stability. Formation of mullite is therefore critical if a dense ceramic that can develop its high-temperature potential is to be achieved [8, 9].

Mullite contains a wide range of Al toSi ratios based on the solid solution $Al_{4+2x}Si_{2-2x}O_{10-x}$, where x ranges from about (0.2-0.9) (about 55 to 90 mol% Al_2O_3) [10].

Compared with other ceramic materials, alumina Al_2O_3 has advantages such as physical, chemical and thermal properties, and it is widely used for abrasives, fire bricks and integrated circuits (IC). It also has excellent mechanical properties, including high hardness, excellent mechanical properties and high tensile strength chemical and thermal stability at a high level.

More than 45 million tons of Alumina are industrially produced worldwide, mainly by the Bayer process using bauxite, with about 40 million tons consumed for refining aluminum. In addition, about (5 million tons) chemical grade alumina is produced and used for various purposes [11].

Titanium dioxide (TiO_2) also known as (Titania), titanium white is the name given to it when used as a pigment. Ilmenite, rutile and anatase are the main sources of the Titania. This occurs naturally in the form of rutile, anatase and brookite. The most common form of ores containing titanium dioxide is ilmenite, the main source of Titania. The second most common

form is rutile, which contains 98% titanium dioxide in the ore [12].

The aim of this work is to study the effect of silica fume on the mixture of alumina and titanium dioxide. Silica fume is a powdery product resulting from gasses evaporated during the production of silicon or ferrosilicon alloys. It is a very fine, non-crystalline, spherical powder with a grain size of up to 0.1µm [13].

Silica fume can be classified as high-grade if it contains more than 88(wt%) SiO_2, or as low-grade if it contains less than. Silica fume produces better pozzolonicity, which can be used in various applications such as concrete admixtures to improve early and late strength. In addition, high quality silica fume can be used to produce large products such as Si_3N_4 powder by carbothermal reduction nitration. It is also used to produce a novel dimensionally stable phase change composite material which is used as a latent heat energy storage system in buildings [14].

2. EXPERIMENTAL PROCEDURE

2.1 Raw materials

The main raw materials for this research are: Pure alumina powder purchased from Huber Engineering Materials Company, pure titanium dioxide powder of rutile type purchased from Interkeram (Hungarian company), and Silica fume is amorphous silicon dioxide SiO_2.

2.2 Raw material characterization techniques

The compositions of alumina, titania and silica fume were investigated by phase identification using a Rigaku Miniflex II X-ray diffractometer (XRD) with CuK radiation (1.54168). Bragg-Brentano geometry is used to operate the diffractometer. Samples were scanned at a speed of 1°/min with a step size of 0.01015° and viewed over a wide range of 2θ-intervals (0-90°). The computer-aided evaluation with the PDF (Powder Diffraction File Database) of the ICDD was carried out with a program especially for this instrument.

The CILAS granulometre 715 instrument was used to measure the particle distribution of all raw materials.

2.3 Specimen preparation and test methods

The raw materials used for the preparation of the ceramic composites were: Al_2O_3, TiO_2, SiO_2 (fume). Three mixtures were prepared, the basic mixture with (80 wt%) alumina and (20 wt%) titanium dioxide and the other two mixtures by adding silica fume to the basic mixture in two proportions (5 and 10 wt%) (Table 1). The prepared mixtures were processed with a planetary ball mill (RETSCH PM 400) for 20 minutes at speed 150 rpm with silica balls. Cylindrical specimens with a diameter of about 25 mm were then prepared from the milled powders by uniaxial pressing at a pressure of 100 MPa. The prepared specimens were sintered for 4 hours at temperatures of 1200℃ in a programmable high-temperature furnace at a heating rate of 5℃/min. The presintered samples were then sintered in air for 4 hours at a high temperature of 1400℃ and a heating rate of 5°C/min. The samples then cooled to room temperature in the oven. Figure 1 shows the steps for fabricating the ceramic composite specimens.

Table 1. Percentages samples composition

Sample code	Chemical composition (wt%)
AT0	80 alumina + 20 Titania
ATS5	76 alumina + 19 Titania+ 5 silica fume
ATS10	72 alumina + 18 Titania+ 10 silica fume

2.4 Techniques for characterizing the ceramic composite specimens

The bulk density of the ceramic composite samples was determined by measuring mass and volume. Water absorption WA (wt%) and apparent porosity P (vol%) were measured.

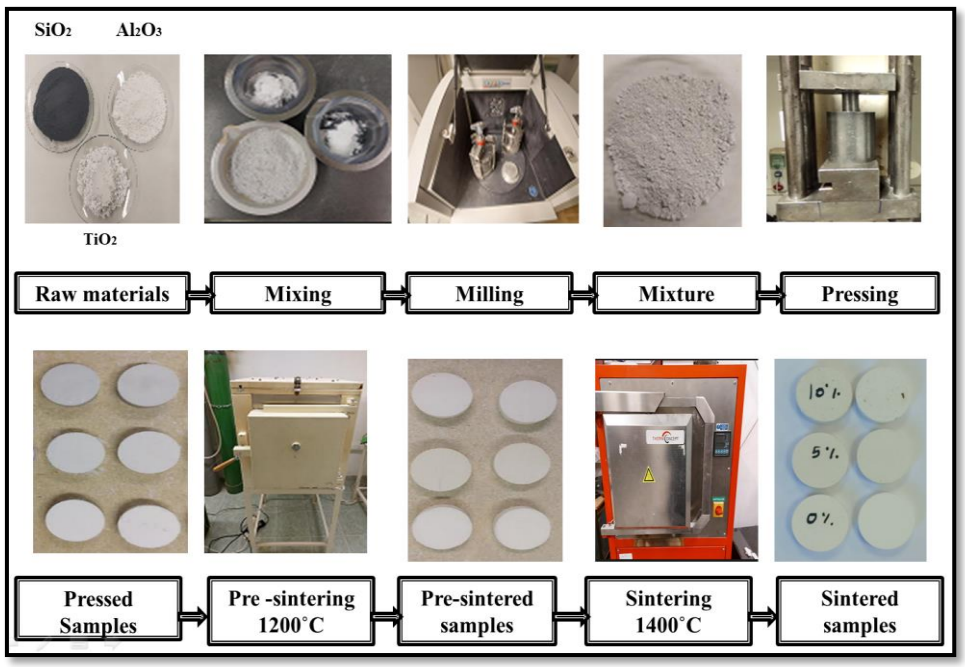

Figure 1. Flowchart describing the steps to produce the ceramic composite specimens

The samples were dried to a constant weight D and then soaked in distilled water for 24 hours at room temperature to measure the wet weight M when the sample is saturated with water and the suspended weight S when the sample was floating in water, according to Archimedes' law.

The test was performed on five representative specimens. The water absorption, measured according to Eq. (1) and the apparent porosity according to Eq. (2):

$$WA = \left(\frac{M - D}{D}\right) \times 100; [\%] \quad (1)$$

$$P = \left(\frac{M - D}{M - S}\right) \times 100; [\%] \quad (2)$$

The volume shrinkage after sintering (1400°C) of the ceramic samples was determined by measuring the volume of the sample before sintering (V_0) and the volume of the sample after sintering (V_1) according to Eq. (3):

$$VS = \left(\frac{V_0 - V_1}{V_1}\right) \times 100; \ [\%] \quad (3)$$

The phase transformation and composition of the ceramic composites after presintering and sintering were investigated using Rigaku Miniflex II X-ray diffractometer (XRD). Microstructural properties and phase identification were performed using scanning electron microscope (SEM). The thermal conductivity of the fabricated ceramic composite samples was measured using a C-Therm TCi thermal conductivity analyzer and a transient plane source.

The C-Therm TCi Thermal Conductivity Analyser is a state-of-the-art thermal property characterization instrument based on modified transient plane source technology. The sensor is highly sensitive and requires careful handling during use and operation. The limitations of the test for the ceramic sample are minimum thickness (5 mm) and temperature range (-50 to 192°C), the surface of the sample was covered with conductive materials, and then the sample was placed on the sensor. The test was performed at room temperature (24.06°C) and the specified voltage was (3504 mV).

3. RESULTS AND DISCUSSION

3.1 Characterization raw materials

Figure 2 shows the X-ray diffraction of the alumina powder, with all peaks indicating the presence of single-phase corundum (α-alumina) without impurities. X-ray diffraction analysis of the titania powder is also shown in Figure 3, with the many strongest peaks indicating the presence of rutile without impurities. Figure 4 shows X-ray diffraction of silica fume indicating the presence of amorphous silica and containing a small peak indicating the polymorphic silica phase cristobalite.

The particle size of titanium dioxide and silica fume was measured with a granulometry device. Only a small percentage of the powders could be measured, about 5% of which had a particle size of 1µm, indicating that the partial size of the powders is ≥1µm, while the granulometry device limits the measurement range (1µm -192µm). The alumina particle size was measured as shown in Figure 5.

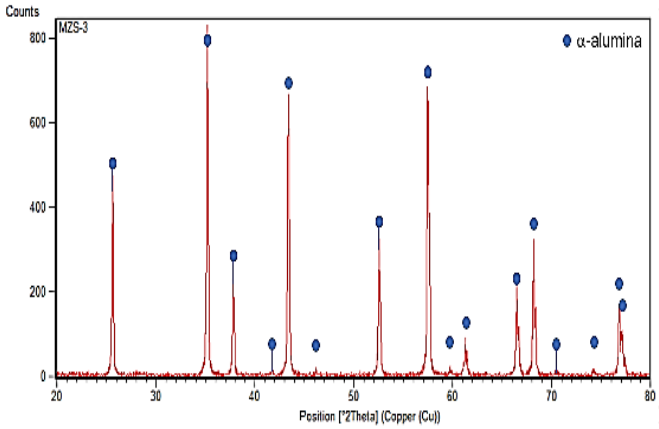

Figure 2. X-ray diffraction of alumina

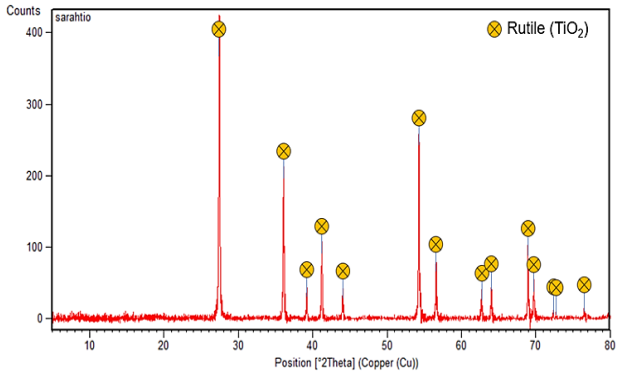

Figure 3. X-ray diffraction pattern of titanat

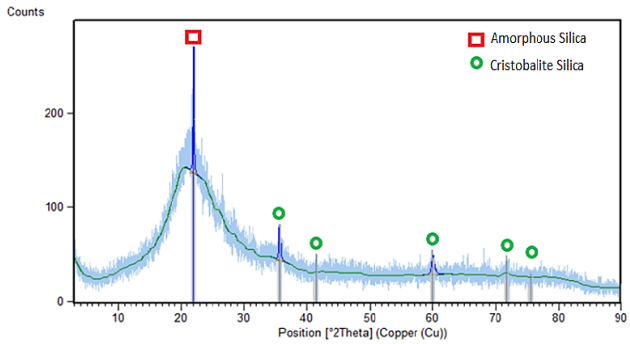

Figure 4. X-ray diffraction of silica fume

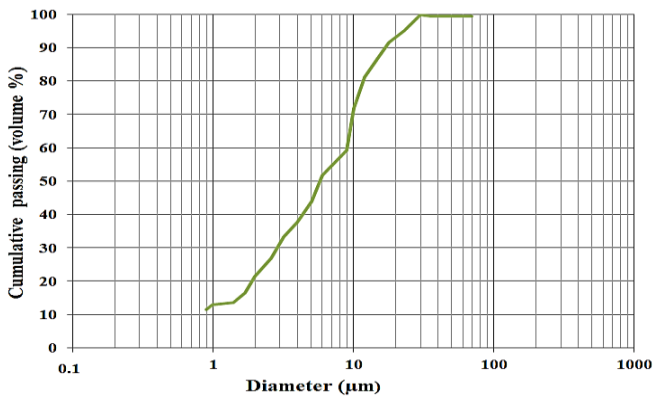

Figure 5. Particle size distributions of alumina

3.2 Characterization results of the produced specimens

3.2.1 XRD investigations of the sample

Figure 6 shows the results of the X-ray diffraction measurements. X-ray diffraction analysis for the ATS5 and ATS10 samples presintered at 1200℃ shows the appearance of crystalline silica. Amorphous silica is transformed into cristobalite by crystallisation (amorphous silica → quartz → cristobalite) at 1400℃. Therefore, in pre-sintered samples were not happened any reaction between the raw materials [15].

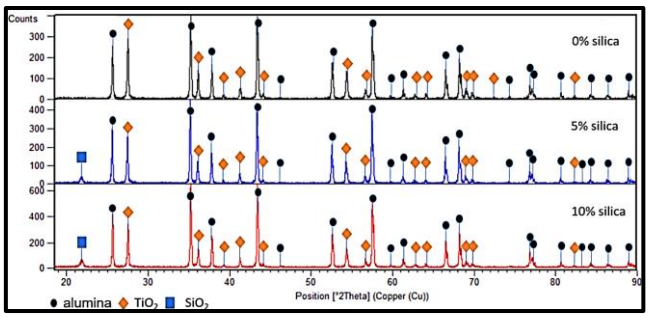

Figure 6. X-ray diffraction patterns of the pre-sintered 1200℃ samples

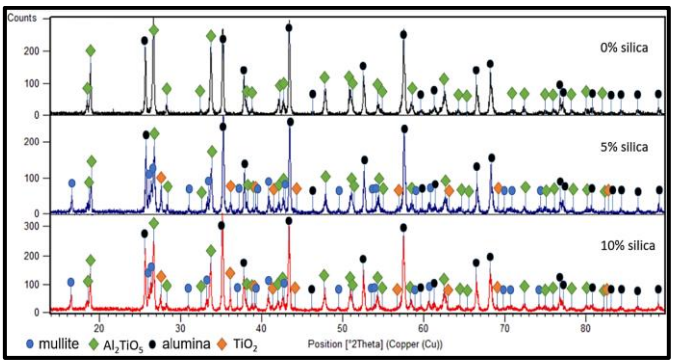

Figure 7. X-ray diffraction patterns of the 1400℃ sintered sample

As shown in Figure 7 the XRD results of the samples sintered at 1400℃ show that in the samples AT the peaks indicate the formation of Al_2TiO_5 and some other peaks indicate the presence of alumina residues, while the X-ray diffraction analysis for the samples ATS5 and ATS10 with the silica fume additions shows, that the same percentage of Al_2O_3 reacted with SiO_2 to form a mullite phase and another percentage of Al_2O_3 reacted with TiO_2 to form an aluminum titanate, and the other peaks found indicate the presence of a minimum of Al_2O_3 and TiO_2 residues.

3.2.2 Scanning electron microscope (SEM) of samples

The scanning electron micrographs of sample AT0 show the nature of the particle shape and size. They are irregularly shaped particles due to the formation of Al_2TiO_5. The average grain size of Al_2TiO_2 was measured to be about 700 nm. The appearance of unreacted Al_2O_3 in the matrix is caused by the crystallization of Al_2TiO_5 grains, followed by the diffusion of the reactant residues through the matrix [16], as shown in Figure 8 (a).

The microstructure of samples ATS5 and ATS10 shows the formation of Al_2TiO_5 and mullite phases and the presence of unreacted Al_2O_3 in the matrix. In the sintered bodies, the grain size of the microstructure is up to 500 nm for sample ATS5 and up to 1000 nm for sample ATS10. This is due to the drag caused by small amounts of the liquid phase that compacts the material, while larger amounts cause excessive grain growth that is detrimental to mechanical performance [17]. Scanning electron micrographs of these samples show a large number of chains with small grain sizes and a tiny minority of whiskers, as shown in Figure 8 (b), (c).

3.2.3 Thermal conductivity of samples

The values of thermal conductivity as a function of composition and of the samples sintered at 1400°C show in Figure 9. That it decreases with increasing silica fume content. Thermal conductivity has a linear relationship with density. The lowest value of thermal conductivity (1.4 W/m.k) was determined for the ATS10 samples with (10 wt%) silica fume content, which had a high density compared to the others.

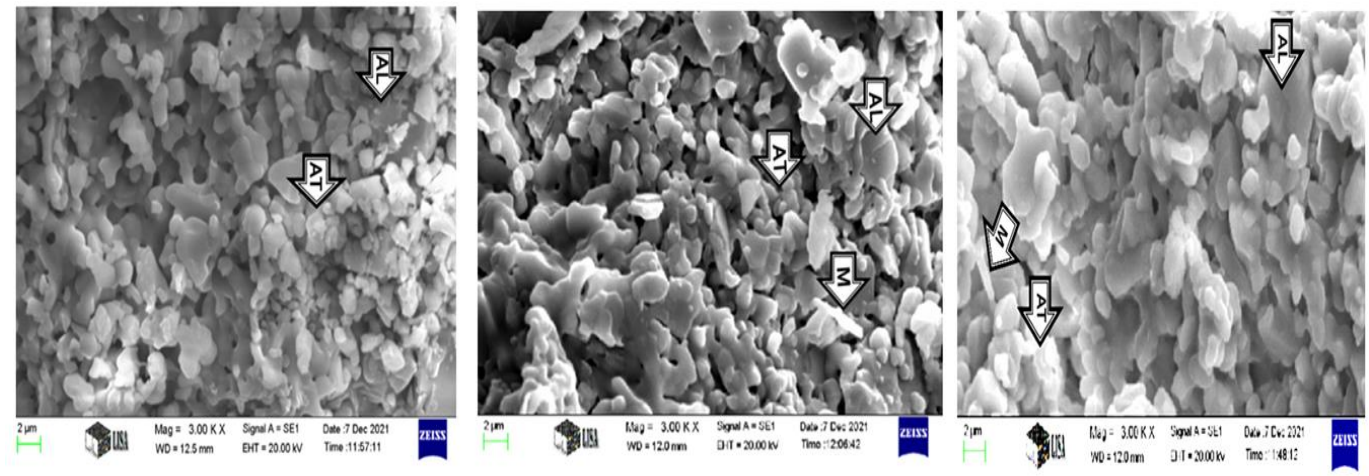

(a) (b) (c)

Figure 8. Scanning electron micrographs of the surface of the samples sintered at 1400°C for 4hours at magnification (3.0KX) (a) AT, (b) ATS5 (c), ATS10. (AL: Alumina, AT: Aluminum Titanate, M: Mullite)

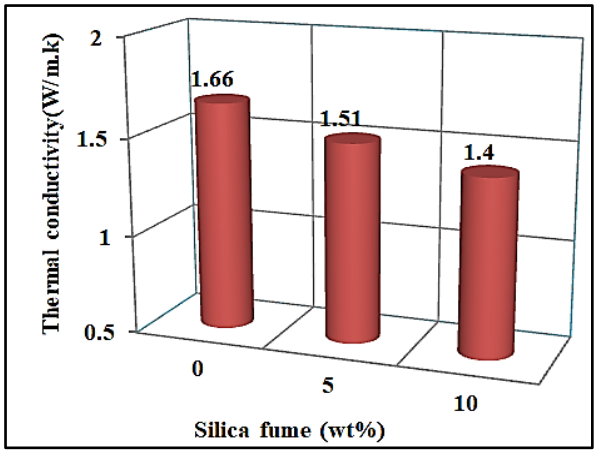

Figure 9. Thermal conductivity of the ceramic composite specimens

3.2.4 Physical properties of the samples

The volume shrinkage after sintering of the samples decreases with increasing alumina content, because alumina has higher thermal stability, resulting in less formation of a liquid phase and less atomic diffusion. The lowest shrinkage was observed for sample AT0 (see Figure 10).

Table 2 shows the physical properties of the samples. The average values of apparent porosity and water absorption of ceramic samples as a function of composition and sintering method. In this work, the apparent porosity shows a minimum value of (20vol%) with a minimum water absorption of (7wt%) for sample ATS5. This is due to the formation of a liquid phase that densities the material, A small percentage of silica fume results in a slight increase in density; however, a larger percentage of silica fume results in increased growth of the grain, which is detrimental to an increase in porosity.

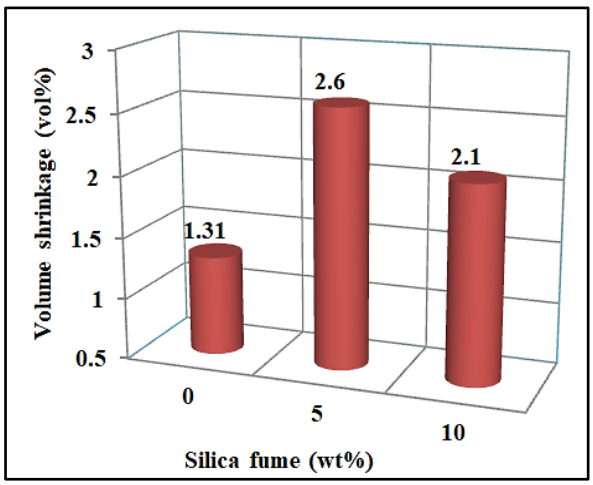

Figure 10. Volume shrinkage of the ceramic composite specimens

Table 2. The physical properties results

Samples code	Apparent porosity (vol. %)	Water absorption (wt. %)	Density (g/cm^3)
AT0	29	10.46	2.60
AT5	20	7.00	2.51
AT10	24	9.50	2.49

One factor that affects the density of a sample is the density of the phases that form during sintering. For example, the average density of mullite (3.16-3.22 g/cm^3) is lower than the average density of aluminum titanate (3-3.4 g/cm^3) [18, 19]. So the density of these samples decreases with increasing silica content as the mullite phase forms.

4. CONCLUSION

Alumina titanate / mullite composites were prepared using alumina titanate as the raw material base with the addition of silica fume. The addition of 5 wt% silica fume can stabilize alumina titanate and improve the development of microstructure, which consists of small grains, while these samples have lower apparent porosity of 20 vol% and lower water absorption 7 wt% but when the addition of 10 wt% silica fume leads to grain growth, which negatively affects the physical properties. Sample AT0, prepared without silica fume addition, had lower thermal conductivity (1.4 W/m.k).

ACKNOWLEDGMENTS

Prof. Dr. László A. Gömze, who established the Ceramic Materials and Silicate Engineering Programmed at the University of Miskolc and recently passed away, was very supportive of this work; may his soul rest in peace.

REFERENCES

[1] Wohlfromm, H., Moya, T.S., Pena, P. (1990). Effect of $ZrSiO_2$ and MgO additions on reaction sintering and properties of Al_2TiO_5 based materials. J. Mater. Sci., 25: 3753-3764. https://doi.org/10.1007/BF00575415

[2] Bachmann, J.L. (1948). Investigations of properties of aluminium oxide and some aluminuos materials. Ph.D Thesis, Pennsylvania State University.

[3] Jung, J., Feltz, A., Freudenberg, B. (1993). Improved thermal stability of Al-titanate solid solutions. Ceram. Forum Int., 70(6): 299-301.

[4] Kim, I.J. (1991). Thermal shock resistant and mechanical properties of aluminum titanate-mullite and powder preparation by solgel process. Dissertation, RWTH Aachen, Germany.

[5] Sarkar, N., Park, J.G., Mazumder, S., Aneziris, C.G., Kim, I.J. (2015). Processing of particle stabilized Al_2TiO_5–$ZrTiO_4$ foam to porous ceramics. J Eur Ceram Soc., 35(14): 3969-3976. https://doi.org/10.1016/j.jeurceramsoc.2015.07.004

[6] Kurovics, E., Kulkov, A.S., Ibrahim, J.E.F.M., Kashin, A.D., Pala, P., Nagy, V., Kulkov, S.N., Gömze, L.A. (2021). Mechanical properties of mullite reinforced ceramics composite produced from kaolin and corn starch. Journal of Silicate Based and Composite Materials, 73(4): 149-153. https://doi.org/10.14382/epitoanyag-jsbcm.2021.22

[7] Mah, T., Mazdiyasni, K.S. (1983). Mechanical properties of mullite. J. Am. Ceram. Soc., 66(10): 699-703.

[8] Lee, W.E., Rainforth, W.M. (1994). Structural Oxides I: Al_2O_3 and Mullite in Ceramic Microstructures Property Control. Processing Chapman and Hall, London, pp. 290-316.

[9] Kurovics, E., Kotova, O.B., Ibrahim, J.F.M., Tihtih, M., Sun, S., Pala, P., Gömze, L.A. (2020). Characterization of phase transformation and thermal behavior of Sedlecky Kaolin. Építőanyag – JSBCM, 72(4): 144-147. https://doi.org/10.14382/epitoanyag-jsbcm.2020.24

[10] Schneider, H., Schreuer, J., Hildmann, B. (2008). Structure and properties of mullite—A review. Journal of the European Ceramic Society, 28(2): 329-344. https://doi:10.1016/j.jeurceramsoc.2007.03.017

[11] Nakano, K. (2001). Alumina powders and their prices. Ceramics, 36(4): 248-253.

[12] Greenwood, Norman N., Earnshaw, A. (1984). Chemistry of the Elements. Oxford Pergamon Press, pp. 1117-1119.

[13] Chen, J.H., Li, T., Li, X.P., Chou, K.C., Hou, X.M. (2016). Morphological evolution of low-grade silica fume at elevated temperature. High Temperature Materials and Processes, 36(6). https://doi.org/10.1515/htmp-2015-0206

[14] Wang, Y., Xia, T.D., Zheng, H., Feng, H.X. (2011). Stearic acid/silica fume composite as form-stable phase change material for thermal energy storage. Energy and Buildings, 43(9): 2365-2370. https://doi.org/10.1016/j.enbuild.2011.05.019

[15] Zinad, R.S., Merzah, A.S., Mohammed, S.K. (2019). Studying the physical and mechanical properties of porcelanite: Lithium metasilicate composite as a dental veneer material. IOP Conference Series: Materials Science and Engineering, 518(3). https://iopscience.iop.org/article/10.1088/1757-899X/518/3/032010

[16] Guedes-Silva, C.C., de Souza Carvalhob, F.M., FerreiraLuis, T.D.S., Genova, A. (2016). Formation of aluminum titanate with small additions of MgO and SiO_2. Materials Research, 19(2): 384-388. http://dx.doi.org/10.1590/1980-5373-MR-2015-0498

[17] Thomas, H., Stevens, R. (1989). Alumina titanate - A literature review. Part. 2 Engineering Properties and Thermal Stability. Br. Cer. Trans. J., 88: 184-1.

[18] Dan, M., Zhuang, G.H., Li, X.X., Tao, H.R., Hui, Y.H. (2004). The characteristics of carbonaceous species and their sources in PM2.5 in Beijing. Atmospheric Environment, 38(21): 3443-3452.

[19] Rahman, S., Freimann, S. (2005). The Real Structure of Mullite. In Mullite, ed. H. Schneider and S. Komarneni. Wiley-VCH, Weinheim, pp. 46-70.

NOMENCLATURE

WA	Water absorption (wt%)
P	Apparernt porosity (vol%)
VS	VoLume shrinkage (vol%)